GOCE gravity gradients: a new satellite observable

Bouman J. (1), Stummer C. (2), Murböck M. (2), Fuchs M. (1), Rummel R. (2), Pail R. (2), Gruber T. (2), Bosch W. (1), Schmidt M. (1)

(1) Deutsches Geodätisches Forschungsinstitut, München

(2) Institut für Astronomische und Physikalische Geodäsie, Technische Universität München

Introduction

The GOCE satellite was launched on March 17, 2009. It is the first mission of ESA's Living Planet Programme and the first satellite with a gravitational gradiometer. GOCE aims at the determination of the stationary part of the Earth's gravity field and geoid with maximum accuracy and spatial resolution (*ESA 1999*). The gradiometer data are essential to achieve this aim. Thus, the first step in GOCE data analysis should be to look into the characteristics of this new data type. Our goal therefore is to obtain a comprehensive understanding of signal and error characteristics of the individual measured gravitational gradients (GGs). This should be the basis of their use in science and application.

In order to get a full understanding of the signal and error characteristics of the GOCE gravity gradients they are studied at four different levels. The first one is gradiometer internal calibration as a pre-requisite in the further processing of the gradiometer data. Once calibrated measurements are available they can be analyzed spectrally and gravity field analysis can be performed. The second level is therefore analysis of the gradiometer data. The GOCE gravity gradients are given in the instrument frame. The analysis of the gravity gradients may require rotation of the GOCE GG to other local reference frames, which represents the third level. This is done with GOCE data only and - in order to strengthen the long wavelength parts - with a combination of recent GRACE gravity models. The goal must be minimum loss of accuracy due to the contribution from the weaker gradient components. The fourth level is gravity gradient validation with satellite altimetry. The high precision and high sample rate of satellite altimeter data permits comparison of gravity gradients derived from satellite altimetry and GOCE gravity gradients.

Gradiometer internal calibration

Gravitational gradiometry based on the principle of differential accelerometry requires the six three-axis accelerometers to have the same scale and to be perfectly aligned. The real instrument can approximate this ideal at most up to a high level of accuracy. Thus, calibration is the central condition for any correct use and interpretation of the gradiometric measurements. Calibration on ground is diffcult due to the presence of g. Therefore calibration is carried out using random shaking of the instrument by a set of cold gas thrusters, (*Cesare and Catastini 2008*), which is called in-flight or internal calibration. Two algorithms have been developed to retrieve the calibration parameters, one by ALENIA and an alternative one by engineers of ESA-ESTEC (*Cesare and Catastini 2008, Lamarre 2008*). Both algorithms determine the calibration parameters iteratively and rely on semi-empirical processing steps that are not fully understood (*Bouman et al. 2008*).

In the nominal processing, the inverse calibration matrices (ICMs) determined by the ESA-ESTEC method from the previous shaking are applied. It was found that some elements of

the ICM from two consecutive shakings (e.g. the shakings of October 2009 and of January 2010) show a significant variation with time. In addition, one observes a slight degradation in time (from October 2009 to January 2010) of the gravity gradient performance when analysing the GGT trace.

To check whether it is possible to avoid this degradation of the GGT trace performance with time, four simulation scenarios have been performed. Since in particular the differential scale factor of accelerometer pair 25 in Y-direction (dSF25y) shows a significant variation with time, the effect of linear interpolating the corresponding ICM element is investigated. Moreover the impact an alternative method for angular rate reconstruction (*ARR, Stummer et al. 2010*) is analysed. For each of the four scenarios, the GGs from 31 October to 31 December 2009 have been reprocessed, using an autonomous implementation of the nominal EGG Level 1b processor:

1) As reference, the original GGs have been reprocessed with the nominal method for ARR and using the nominal (previous) ICM.
2) As 1) but with interpolation of the ICM element corresponding to dSF25y.
3) Instead of the nominal method for ARR, the Wiener ARR method was used. The nominal ICMs have been applied.
4) Again, the Wiener method for ARR was used, but this time with interpolation of the ICM element corresponding to dSF25y

Figure 1 illustrates the trace performance of the four sets of gravity gradients from scenarios 1) to 4) at a day (27 December 2009) that is far away in time from the October calibration and thus the variation of dSF25y with respect to this calibration is expected to be large.

One can notice that:

– When using the nominal ARR method, there is only a small improvement of the GGT trace performance due to ICM interpolation

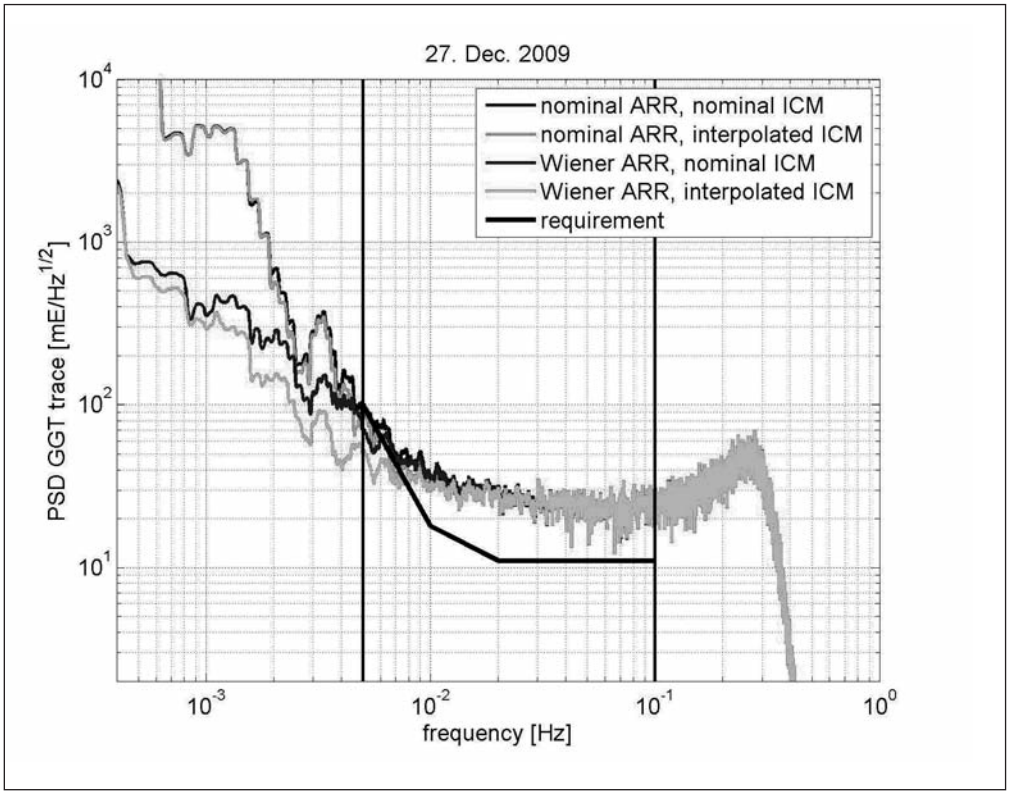

Figure 1: PSD of GGT trace, effect of ICM interpolation (dSF25y) using nominal and Wiener method for ARR

(upper black vs. grey curves) for frequencies at the lower end of the MBW (5 mHz).

– With the Wiener method for ARR (using nominal ICM, lower black curve), the GGT trace performance improves significantly with respect to the nominal ARR method (two upper curves). The improvement is largest for low frequencies and is to a smaller extent still present for frequencies up to 7 mHz.
– The GGT trace performance is best when the Wiener method for ARR is used and the ICM element corresponding to dSF25y is interpolated (lower grey curve).

Thus, it is confirmed that a change of an accelerometer scale factor can have a significant impact on the accuracy of the gravity gradients. Moreover, it is possible to compensate for this effect to some extent by linear interpolation of the corresponding ICM element using the Wiener method for ARR. When the nominal method for ARR is used this positive effect of ICM interpolation cannot be achieved.

Analysis of the gradiometer data

Since GOCE is the first satellite mission ever with a gradiometer on board, the analysis of these data with noise is very important. The spectral characteristics of the gradiometer measurements can be analyzed in several ways. One option is to use the redundancy within the accelerometers and the gradiometer as a whole, to check the individual components against each other. Each of the 6 three-axis GOCE accelerometers has two ultra-sensitive (US) axes and one less sensitive (LS) axis. The two US axes measure the Control Voltages (needed to keep the accelerometers proof mass stable) with 2 electrode pairs, the LS axes have 4 electrode pairs. Therefore, in total there are 6*8 = 48 electrode-pairs.

To check the performance of each of these electrode pairs, the nominal GOCE Level 1b processing has been rerun, replacing the measurements of one specific electrode pair with the measurements of the corresponding pair along the same axis. In Figure 2 the impact of

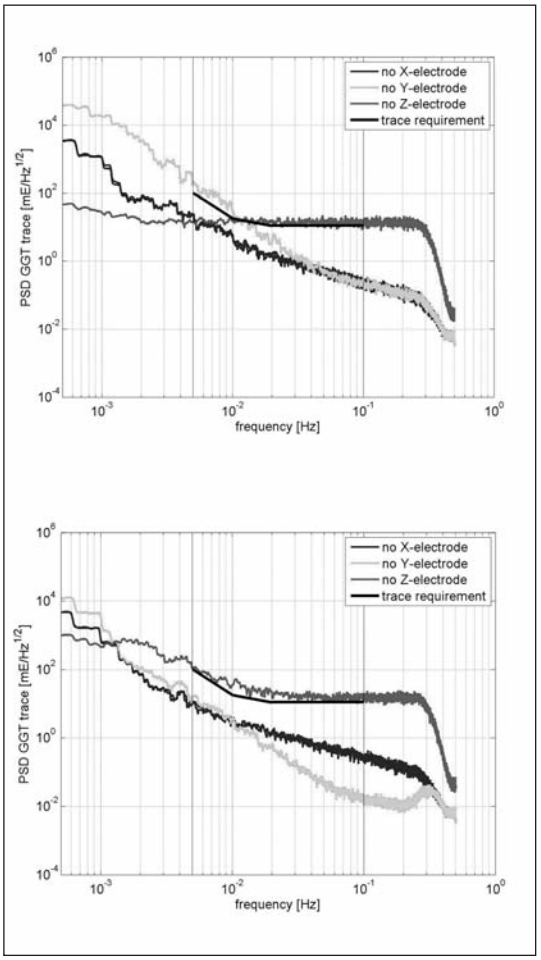

Figure 2: Impact on GGT trace due to the replacement of individual Control Voltages of accelerometer 1 (top) and of accelerometer 2 (bottom)

the replacement on the GGT trace is shown. For a better visualisation, always the PSD of the difference between the specific new GGT trace and the nominal one (using all measurements) has been computed. One can notice two things. First, the replacement of measurements along one specific axis always causes a similar impact on the GGT trace. Therefore, it can be excluded that there is one electrode with a particular bad performance. Second, the impact on the GGT trace depends on the axis on which the replacement is done. E.g. the replacement of a Z-electrode (in the Accelerometer Electrode System Reference Frame (AESRF), red curves) has a significant impact on the GGT trace throughout the complete gradiometer measurement band width (MBW). Table 1 gives a detailed overview of the impact of electrode replacements on the individual gradients.

Table 1: Impact on gradients due to replacement of Control Voltages

Sensi-tivity	Arrange-ment	ACC	Axis in AESRF	Axis in GRF	Impact on	Frequency range
US	In-line	1/4 2/5 3/6	Z	X	V_{xx}	Within MBW
			Z	Y	V_{yy}	
			Z	Z	V_{zz}	
US	Trans-versal	1/4	Y	Z	$\dot{\omega}_y$	Lower MBW
		2/5	Y	X	$\dot{\omega}_z$	Not significant
		3/6	Y	X	$\dot{\omega}_y$	Lower MBW
LS	Trans-versal	1/4	X	Y	$\dot{\omega}_z$	Not significant
		2/5	X	Z	$\dot{\omega}_x$	
		3/6	X	Y	$\dot{\omega}_x$	

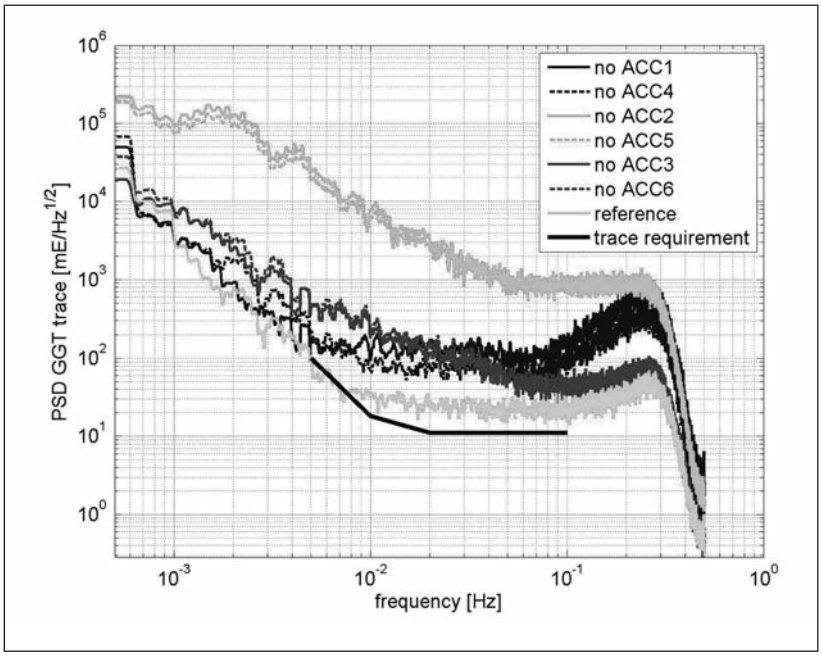

Figure 3: Impact on GGT trace due to replacement of complete accelerometers

Additionally, 6 sets of GGs have been computed, replacing one accelerometer by a virtual accelerometer, which is formed by the common-mode accelerations of the corresponding remaining accelerometers. In Figure 3 the PSDs of the GGT trace for all six cases of accelerometer replacement are shown. Again, one can notice two things. First, the impact on the GGT trace is similar for the accelerometers on the same gradiometer arm. Second, the impact is depending on the axis on which the replacement is done. The GGT trace degrades most, if an accelerometer on the Y-axis, accelerometer 2 or 5 (two upper curves), is replaced, because these accelerometers are the only ones with US axes in Y direction, which is the main measurement direction in this case. Therefore, the Y-direction of the corresponding virtual accelerometer can only be built from LS measurements.

Spectral characteristics of the diagonal gradiometer components

Theoretically the gravity gradients individually

as well as certain well defined combinations show typical spectral characteristics, see e.g. (*Rummel and van Gelderen 1992, Rummel 1997*). In reality these theoretical properties will only be met to a certain extent. This is due to measurement noise, imperfect calibration, less sensitive accelerometer components and to rotational effects. Thus, these spectral characteristics are an important tool for the assessment of the quality of measured gradients. Further insight in the GOCE gravity gradient characteristics is obtained by their global behaviour in terms of spherical harmonic coefficients by the semi-analytic method (*Sneeuw 2000, Pail and Plank 2002, Wermuth et al. 2006, Pail et al. 2007*). It is feasible to use single gravity gradient components as well as various combinations of gravity gradient components for global spectral analysis, for the first time using real data.

Each individual gradiometer component has its own spectral strength and weakness. The actual spectral characteristics are analyzed, employing spherical harmonic (SH) analysis on the three diagonal components. The observations used are GOCE data from November and December 2009. A semi-analytical approach leads iteratively to a consistent adjustment resulting in SH coefficients and a Block-Diagonal Variance-Covariance matrix. The estimated standard deviations of this solution can be seen in Figure 4 (top) in the spherical harmonic (SH) domain. Typical SH error characteristics of GOCE GG can be seen. The inclined orbit, which provides no observations over the poles, leads to large errors around the zonal coefficients. The sensitivity for lower degrees is quite low and a near isotropic behaviour can be observed in the higher degrees (i.e. main dependency of the errors of the SH degree and not of the SH order). Bright stripes around multiples of the SH order 16 for low degrees are noticeable as well, which are characteristic for high noise at multiples of the orbit frequency. It is useful to compare the estimated standard deviations with the differences of the estimated SH coefficients and the coefficients of an existing gravity field model (here EIGEN-5C) (Fig. 4 middle). These coefficient differences lead to comparable SH structures. A different look at this comparison is provided by the median per SH degree of these two SH spectra (Fig. 4 bottom). The median is used because it is not sensitive to the very high errors around the zonals affected by the polar gap. As EIGEN-5C is a combined model from five years GRACE and LAGEOS data we assume it to be better in the lower degrees than GOCE. Therefore the differences in these degrees can

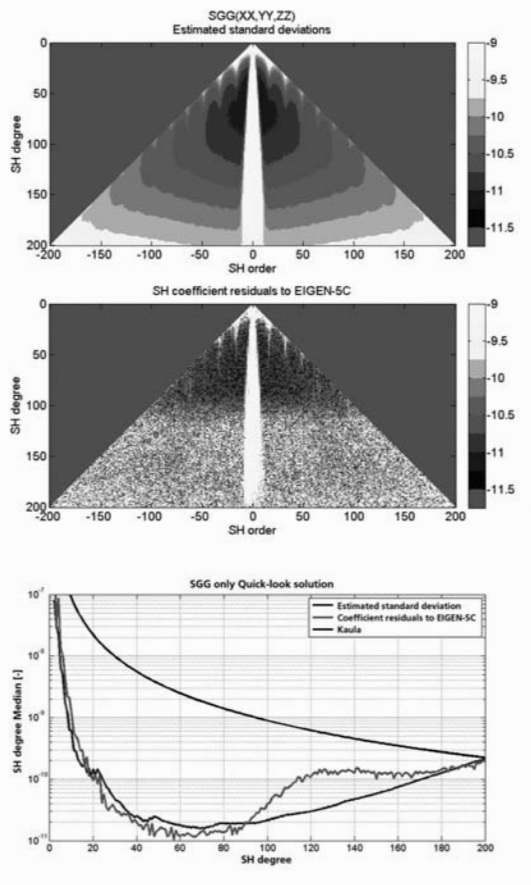

Figure 4: Top: estimated standard deviations of a semi-analytical gravity field estimation of GOCE's GGs of November and December 2009 (log10). Middle: Differences between the estimated SH coefficients and the coefficients of EIGEN-5C Bottom: SH degree median of the two upper SH coefficients

be assumed to be mainly errors. As the median of the estimated standard deviations is quite close to the median of the coefficient differences it can be assumed that the observations are processed consistently and lead to realistic errors for GOCE's GGs.

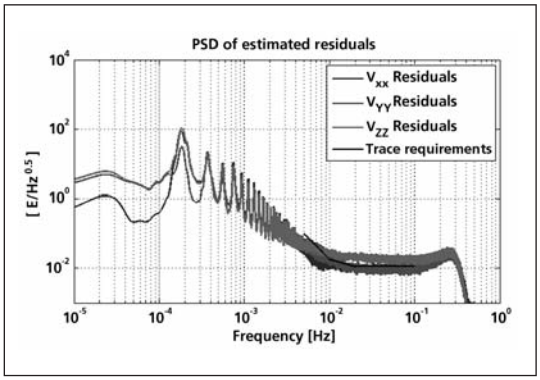

Figure 5: PSD of the estimated residuals of the three diagonal components

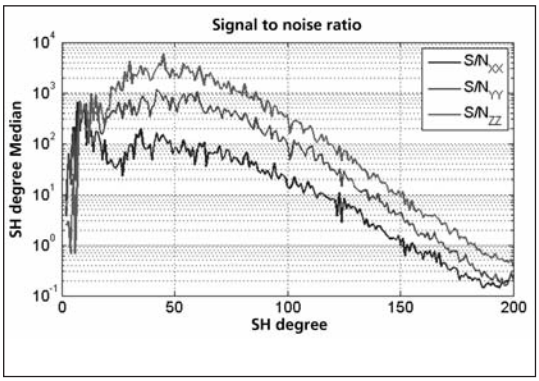

Figure 7: SH degree median of the signal to noise ratio of the three diagonal components

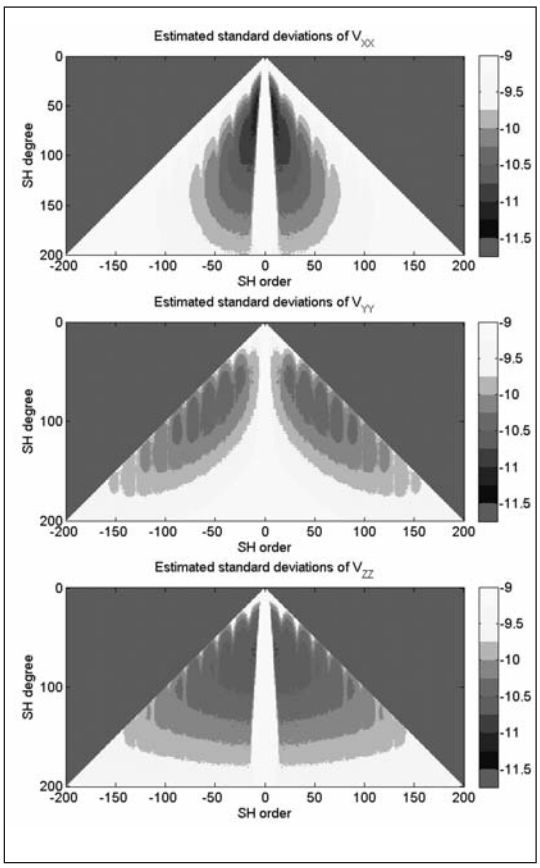

Figure 6: SH error spectra of the three diagonal components (top: XX, middle: YY, bottom: ZZ) (log10)

This analysis provides the estimates of the observation residuals as well. A spectral representation of these residuals shown in Figure 5 as PSDs. Derived from a consistent processing of the combination of the three diagonal components of GOCE's GGs to SH coefficients, these PSDs gives a realistic error characteristic of each of the 3 components in the frequency domain. One can notice two things. All 3 components show similar noise behaviour with frequency. Large peaks occur at multiples of the orbit frequency. The noise level for frequencies above 10 mHz is nearly constant (white noise) and around 10 mE/Hz$^{0.5}$. Nevertheless some differences can be observed. The noise level of V_{ZZ} in the upper frequency range is nearly two times larger than the other two components. At around 10 mHz the V_{XX} component seems to have a lower noise level than the others.

By propagating this noise PSDs in a semi-analytical way onto the SH spectrum one gets the noise behaviour in the SH domain (Figure 6). The peaks in the PSDs are mapped on multiples of the SH order 16 and are visible in bright stripes as in the combined solution. The theoretical characteristics remain in this realistic case. These are the large errors around the zonals (polar gap) and the typical sensitivities for V_{XX} (around the zonals), V_{YY} (sectorials) and V_{ZZ} (near isotropic). Dividing these errors by the SH coefficients of the estimated signal a signal to noise ratio in the SH domain arises. Its median per SH degree can be seen in the right Figure 7. The V_{ZZ}-component has the highest S/N ratio for all SH degrees, the V_{XX}-component the smallest.

Rotation of the gravity gradient tensor

The calibrated gravity gradients, as derived from the GOCE gradiometer, are given in the GRF, the Gradiometer Reference Frame, which

co-rotates with the satellite in its orbit. The GRF is approximately oriented in the radial, along-track, cross-track direction and is governed by the attitude control system. While the location of the measurements is determined using GPS orbit determination, the orientation in inertial space relies on the star sensors. In principle it is therefore possible to rotate the measurements to a local geographical frame. Such a representation would allow a more general analysis and interpretation of the measurements independent of satellite orbit and satellite position.

There are, however, two problems in the transformation of the gravity gradients from the GRF to other frames. First, the rotation of the gravitational tensor from one orthonormal frame to another requires the pre- and post-multiplication of the tensor with a corresponding rotation matrix. Consequently, the tensor components in the rotated system are linear combinations of the components in the original system. Because two of the non-diagonal tensor components are much less accurate than the other components, a rotation to another frame will also make the diagonal components in the transformed frame less accurate (*Müller 2003*). Secondly, the accurate gravity gradients do have high accuracy in the MBW (Measurement Bandwidth), but the error increases for low frequencies. This error tends to leak into the MBW while transforming from GRF to other local frames (*Bouman 2007*).

An algorithm has been developed and implemented to prevent gravity gradient deterioration in the frame transformation. The GOCE gravity gradient signal below the MBW is replaced by signal from a global model to prevent leakage, for example a GRACE or a GOCE quick-look model (*Foerste et al. 2007, Pail and Wermuth 2003*). In addition, the two less accurate gravity gradients in the GRF are replaced by gravity gradients which have been computed from a quick-look GOCE gravity field model.

Dependent on the gradiometer performance the spectral limit of model information and measured GGs has been evaluated using a trade off between signal bandwidth, signal energy and measurement noise. This limit, which is assigned by the filter cut-off frequencies, is important because it gives a value for the long wavelength quality of GOCE data. Due to the impact of rotational effects on the rotated GGs, the cut-off frequency is being derived in the rotated reference frame by an analysis aiming for an optimal ratio between signal and noise energy of the derived GGs. With this analysis the low frequency spectral gradiometer performance can be tested and evaluated.

The tensor rotation of GOCE GGs mixes components derived from model information and measurements which depends on the rotational angle, the spectral signal strength, the gradient axes and the orbit height. The amount of GOCE information in the rotated gradients is an important quantity for local analysis. Two frames are of special interest: the local orbital reference frame (LORF) and the local north oriented frame (LNOF). The LORF X-axis is aligned with the velocity vector of the satellite, the Z-axis is in almost radial direction in the orbital plane and Y-axis complements the right-handed frame. The X-axis of the LNOF points North, the Y-axis West and the Z-axis radial outward.

The ratio of model and GOCE GGs has been used to evaluate the model content present in the rotated gravity gradients in different reference frames. The amount of model information in the rotated gradients is shown in Figure 8 for V_{YY} (LNOF & LORF). As the GRF is aligned within a few degrees with the LORF, the rotations from GRF to LORF are small, whereas the rotation about the yaw axis can be large going from GRF to LNOF. The mean model content in the rotated gradients is summarized in Table 2.

The rotated gravity gradients can be used to validate and evaluate global gravity field models at the GOCE orbit in the LNOF. Especially for the fine scale structures in common global gravity field models such as e.g. the EGM2008 or the EIGEN5C differences are seen globally and particular in regions such as South America,

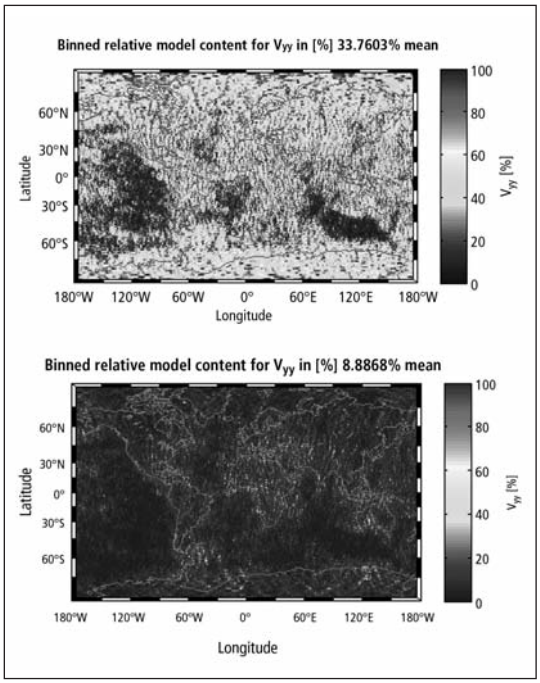

Figure 8: Relative model content in V_{YY} LNOF (top) and LORF (bottom)

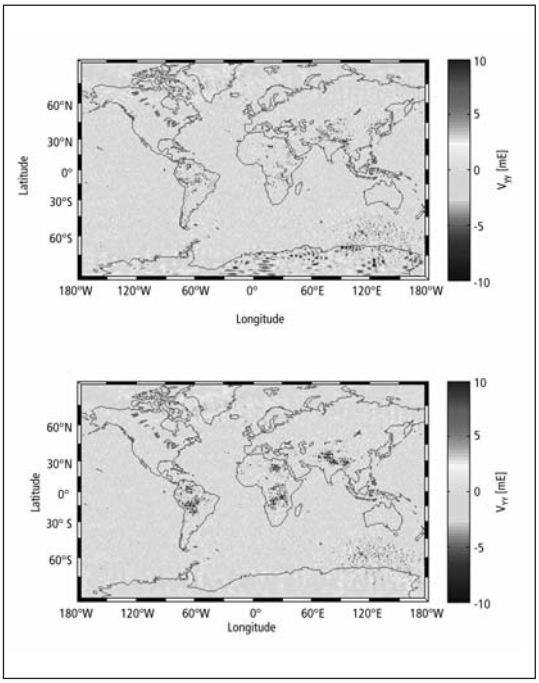

Figure 9: V_{YY} binned averaged differences 31 October 2009 – 11 January 2010: GOCE - EIGEN5C (top), GOCE - EGM2008 (bottom)

Table 2: Mean relative model content in rotated gravity gradients in LNOF and LORF)

GG	LNOF	LORF
V_{XX}	20.8 %	2.6 %
V_{YY}	33.8 %	8.9 %
V_{ZZ}	1.1 %	2.0 %
V_{XZ}	14.2 %	4.2 %

Africa or South Asia, see Figure 9. The measurement anomalies in V_{YY} south of Australia and Northern Canada are a non gravity related GOCE feature, which is probably related to a drift in the gradiometer differential scale factors (see section on gradiometer internal calibration).

Gravity gradient validation with satellite altimetry

Since many years satellite altimetry provides measurements of mean sea level (MSL). MSL nearly coincides with an equipotential surface of the Earth gravity field, the geoid. Deviations between mean sea level and geoid, known as dynamic ocean topography (DOT) are caused by external forcing and remain below ± 1-2 m. The mean curvature of the geoid is proportional to the radial gravity gradient of the disturbing potential (*Heiskanen and Moritz 1967*). It can be shown that the mean curvature of the mean sea level is a very precise measure of the curvature of the geoid (*Bosch 2003, Bouman et al. 2010*). Thus, from the geometry of the mean sea level one can infer the second radial derivative of the disturbing potential. This opens the possibility to use satellite altimetry for the validation of gradients.

GGs may be transformed to any arbitrary reference frame and therefore also to a reference frame aligned with satellite altimeter ground tracks. This opens the possibility to use the single gravity gradient components for modelling and comparison with along track gravity gradient profiles as derived from satellite altimetry, cf. (*Rummel and Haagmans 1991, Khafid 1993*). In addition, at crossover points of altimeter ground tracks the second radial derivative of the gravitational potential can be determined using the along track gravity gradient profiles of ascending and descending tracks (*Rummel and Haagmans 1991*). At crossover points altimetric gravity gradients (radial component) may therefore be used to validate the GOCE radial gravity gradients.

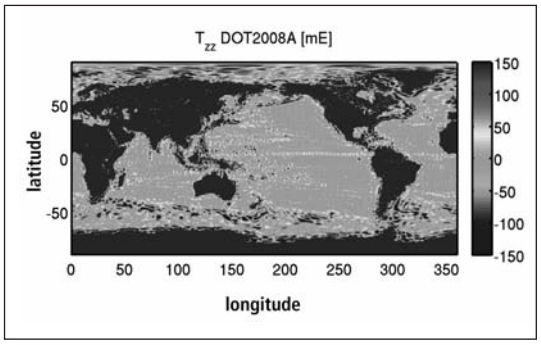

Figure 10: DOT TZZ signal at the Earth's surface computed with DOT2008A

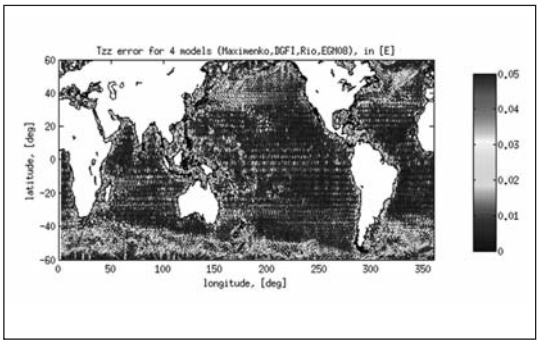

Figure 11: T_{ZZ} RMS differences for 4 different DOT-models

We assessed how large the influence is of neglecting the DOT and thus assuming that MSL is an equipotential surface. The DOT model DOT2008A has been expanded in spherical harmonics (*Pavlis et al. 2008*) and the coefficients have been used to compute the vertical GG with respect to a reference ellipsoid, This DOT TZZ signal is shown in Figure 10 where the colour bar has been set to ±150 mE. For reference: the error in the accurate GOCE gravity gradients is 10 – 20 mE for medium resolutions. The DOT can therefore not be neglected.

Because the DOT cannot be neglected it must either be modeled or estimated simultaneously with, for example, a regional gravity field when satellite altimeter data and GOCE gravity gradients are combined. Different models for the DOT exist and we computed the differences between 4 models. The RMS of these differences, in terms of vertical gravity gradient, is shown in Figure 11. Clearly, the differences between the DOT models are large in regions with the major currents. There are however also regions, such as the Pacific, where the differences between the DOT models are small. Satellite altimeter data in these regions could be used for GOCE validation if the altimeter data are corrected for DOT.

Acknowledgements

This work was sponsored by the German Department for Education and Research (Bundesministerium für Bildung und Forschung) as part of the GEOTECHNOLOGIEN program. Josef Sebera provided the figure on DOT differences.

References

Bosch W (2003) On the combination of altimetry and satellite derived gravity field models. Presented at the IUGG General Assembly, Sapporo, Japan

Bouman J (2007) Alternative method for rotation to TRF. GO-TN-HPF-GS-0193, issue 1.0

Bouman J, Catastini G, Cesare S, Jarecki F, Müller J, Kern M, Lamarre D, Plank G, Rispens S, Veicherts M, Tscherning CC, Visser P (2008) Synthesis analysis of internal and external calibration. GO-TN-HPF-GS-0221, Issue 1.0

Bouman J, Bosch W, Sebera J (2010) Assessment of systematic errors in the computation of gravity gradients from satellite altimeter data. Accepted for publication in Marine Geodesy

Cesare S, Catastini G (2008) Gradiometer on-orbit calibration procedure analysis. Issue 4, GO-TN-AI-0069, Alenia Spazio, Turin

ESA (1999) Gravity Field and Steady-State Ocean Circulation Mission. Reports for mission selection; the four candidate earth explorer core missions, ESA SP-1233(1)

Foerste C, Schmidt R, Stubenvoll R, Flechtner F, Meyer U, Koenig R, Neumayer H, Biancale R, Lemoine JM, Bruinsma S, Loyer S, Barthelmes F, Esselborn S (2007) The GeoForschungsZen-

trum Potsdam / Groupe de Recherche de Géodésie Spatiale satellite-only and combined gravity field models: EIGEN-GL04S1 and EIGEN-GL04C. J Geod. doi: 10.1007/s00190-007-0183-8

Heiskanen W, Moritz H (1967) Physical geodesy. W.H. Freeman and Co.

Khafid (1993) Filtering of satellite altimetry data with optimal smoothing cubic splines. Master's thesis, Faculty of Geodetic Engineering, Delft University of Technology

Lamarre D (2008) Algorithm description: retrieval of gradiometer parameters. Version 2.0 draft, 23/APR/08

Müller J (2003) GOCE gradients in various reference frames and their accuracies. Adv Geosci 1:33–38

Pail R, Plank G (2002) Assessment of three numerical solution strategies for gravity field recovery from GOCE satellite gravity gradiometry implemented on a parallel platform. Journal of Geodesy, 76:462–474

Pail R, Metzler B, Preimesberger T, Lackner B, Wermuth M (2007) GOCE Quick-Look Gravity Field Analysis in the Framework of HPF. In Proceedings of the 3rd International GOCE User Workshop. ESA-ESRIN, Frascati, Italy, 6-8 November 2006, ESA SP-627

Pail R, Wermuth M (2003) GOCE SGG and SST quick-look gravity field analysis. Advances in Geosciences, 1:5–9

Pavlis DE, Holmes SA, Kenyon SC, Factor JK (2008) An Earth Gravitational Model to Degree 2160: EGM2008, Presented at EGU General Assembly 2998, Vienna, Austria

Rummel R (1997) Spherical spectral properties of the earth's gravitational potential and its first and second derivatives. In F. Sansò and R. Rummel, editors, Geodetic Boundary Value Problems in View of the One Centimeter Geoid, volume 65 of Lecture notes in earth sciences, pages 359–404. Springer, Berlin

Rummel R, Haagmans R (1991) Gravity gradients from satellite altimetry. Marine Geodesy, 14, 1–12

Rummel R, van Gelderen M (1992) Spectral analysis of the full gravity tensor. Geophysical Journal International, 111:159–169

Sneeuw N (2000) A semi-analytical approach to gravity field analysis from satellite observations. Reihe C No. 527, Deutsche Geodätische Kommission

Stummer C, Fecher T, Pail R (2010) Improved method for angular rate determination within the GOCE gradiometer processing. Submitted to J Geod

Wermuth M, Rummel R, Földvary L (2006) Mission Simulation and Semi-Analytical Gravity Field Analysis for GOCE SGG and SST. In J. Flury, R. Rummel, C. Reigber, M Rothacher, G. Boedecker, and U. Schreiber, editors, Observation of the Earth System from Space, pages 193–208. Springer